

Modeling of Ultrasound Hyperthermia Treatment of Breast Tumors

Osama. M. Hassan¹, Noha. S. D. Hassan¹, and Yasser. M. Kadah^{1,2}

¹Biomedical Engineering Department, Cairo University, Egypt (E-mail: ossama_hassan@k-space.org)

²Center for Informatics Science, Nile University, Egypt (E-mail: ymk@k-space.org)

Abstract

Ultrasound hyperthermia has become one of the new therapeutic modalities for breast cancer treatment, since ultrasound appears to selectively affect malignant cells without causing any deleterious effects to the surrounding normal tissues. The main objective of this study is to numerically simulate the interaction of therapeutic ultrasound with a multi-tissue type system, and to develop an analytical model for calculating the temperature rise in these tissues due to ultrasound. First, the Finite-Element Method has been used to compute the radiated power density produced by a circular ultrasonic transducer disk, the heat deposition in each of the biological tissues and the 2-D temperature distribution during ultrasound hyperthermia. Second, an analytical model was developed in which a modified heat transfer equation was used to compute temperature profiles in different tissues. The therapeutic transducer was employed at three different frequencies of 0.75, 1.5 and 2.75 MHz and simulations were allowed to run from 180 to 300 seconds, for a focal depth 10 cm below the surface of the breast tissue. Numerical results of the temperature distribution in different tissues were compared with analytical calculations. The results show that employing a transducer at a frequency of 1.5 MHz is the most suitable for a successful ultrasound therapy in this application.

Keywords – *Finite* element modeling, Bio-heat equation, Ultrasound hyperthermia.

1. Introduction

In cancer treatment, hyperthermia became important as it increased significantly the therapeutic success and clinical management. Numerous biological and clinical investigations have demonstrated that hyperthermia in the 40-45°C range can significantly enhance clinical responses to radiation therapy, and has potential for enhancing other therapies, such as chemotherapy, immunotherapy and gene therapy. Furthermore, high-temperature hyperthermia (greater than 50°C) alone is being used for selective tissue destruction as an alternative to conventional invasive surgery. The degree of thermal enhancement of these therapies is strongly dependent on the ability to localize and maintain therapeutic temperature elevations, due to the often heterogeneous and dynamic properties of tissues, most notably blood perfusion and the presence of thermally significant blood vessels, therapeutic temperature elevations are difficult to spatially and temporally control during these forms of hyperthermia therapy. However, ultrasound technology has significant advantages that allow for a higher degree of spatial and dynamic control of the heating compared to other commonly utilized heating modalities.

1.1. Relevant previous work

Various mathematical and analytical approaches have been developed over three decades, so as to aid in an understanding of the interaction of ultrasound with biological tissues and the lesion development during focused ultrasound surgery. First, analytical models calculating heating patterns due to therapeutic transducers were developed. Second computer modeling has been used to determine the temperature distribution of a given treatment and to plan future hyperthermia treatments.

1.1.1. Analytical Model of Ultrasound Hyperthermia

Generally speaking, a number of studies have concentrated on modeling the heating from single exposures from axially symmetrical transducers, such as spherical bowls, and subsequent lesion formation. Pond developed a simple analytical model that broke down the heating volume into a series of cylinders that were used as elemental heat sources [1]. On the other hand, a model for tumor therapy based on the bio-heat equation [2] was developed to calculate intensity patterns by a one-dimensional transformation of the diffraction equation and temperatures were computed using a successive over-relaxation method assuming uniform perfusion [3]. Bing et al developed a model with a simplified ultrasound beam model to examine the optimal driving frequency and

treatable domain formed by the tumor size and tumor depth and to simulate the SAR distribution for the hyperthermia treatment of bone tumor [4].

1.1.2. Numerical Modeling

Computer modeling has been used to determine the likely temperature distribution of a given treatment and to plan the future of hyperthermia treatments. So, the goal of computer simulation is extremely useful in providing a firm scientific basis for the future of clinical investigation of focused ultrasound. Kagawa *et al.* have reported a finite element model to solve the bioheat equation as well as the wave equation. However; the computational burden restricted their model to a two-dimensional solution of steady state [5]. On the other hand, a 3-D finite-element representation of the bioheat equation was implemented with the heat deposition patterns computed assuming a linear propagation model [6]. However, a number of difficulties were encountered such as the extremely high storage requirement and runtime needed to compute the ultrasound field in the required frequency ranges. Finally, a model using the finite-element analysis (FEA) to calculate the temperature rise in tissue from intracardiac ultrasound ablation catheters and to predict the temperature adequate for producing a lesion in the tissue was implemented [7].

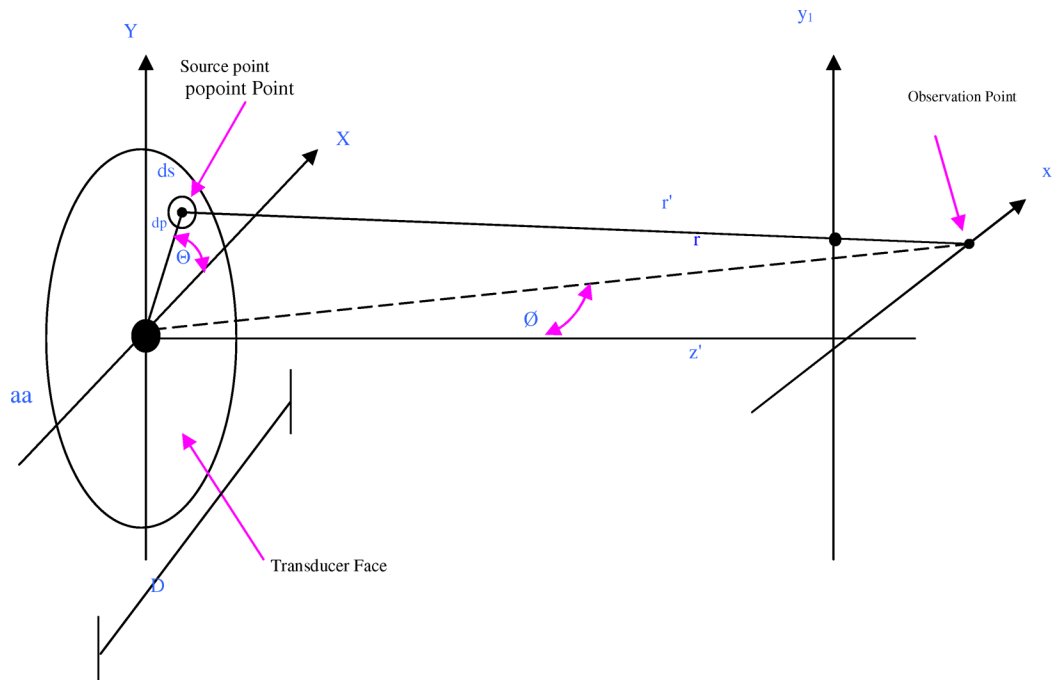


Fig.1. The general coordinates for solving the radiation pattern from a circular ultrasound transducer of radius a and diameter D . dp is the incremental pressure at the observation point due to a spherical wave from a point source of incremental size ds .

In this paper, a 2-D finite-element representation of the bio-heat equation was implemented with the heat deposition patterns computed assuming the absorption and attenuation coefficients being equal at different simulation frequencies and therapy durations. The finite-element method has the advantage over finite difference-based techniques of being able to utilize nonuniform grids, thus allowing for a high rate of spatial sampling in specific areas of interest, and using a low sampling rate in regions known to have minimal heating. In addition, we developed an analytical method to efficiently predict the sound field radiated by an acoustic circular transducer disk and to predict the temperature rise in the regions of interest. Results were subsequently compared with the numerical results computed using a commercially available software COMSOL in an effort to obtain quantitative information on the interaction between high-energy ultrasound and biological tissues.

2. Methodology

2.1. Calculation of the Radiated Power Density Pattern

The geometry for determining the far-field radiation from a circular transducer is given in figure 1. The ultrasound field intensities were calculated from the following equation [8],

$$I(\phi, r, t) = \frac{\pi^2 a^4 u_0^2 Z \sin^2(\alpha t - kr)}{\lambda^2 r^2} \left[\frac{2J_1(ka \sin \phi)}{ka \sin \phi} \right]^2, \quad (1)$$

where J_1 is the Bessel function of the first kind with order 1, a is the radius of the circular transducer, Z is the acoustic impedance of the medium or tissue, k is the wave propagation constant ($k = 2\pi/\lambda$), r is the distance from the source point to the observation point ($r = \sqrt{x^2 + z^2}$ in the far field pattern), u_0 is the aperture excitation, x is the coordinate in the plane of observation, and z is the depth. The velocity u_f of the transducer faces (touching tissue or a bolus of water) at resonance is:

$$u_f = \pm \frac{2e_{ii}E_i}{Z_1 + Z_2}. \quad (2)$$

Here, E_i is the electric field applied, e_{ii} is the material's piezoelectric stress coefficient. Z_1 and Z_2 are the acoustic impedances of the media on either side of the transducer, and the \pm sign denotes that the face velocities are in opposite directions since a resonant vibration mode with an odd number of half-wavelengths was assumed. Since many transducers have air in the region to the rear of the transducer; the acoustic impedance $Z_1 \approx 0$ and equation (2) reduces to,

$$u_f = \frac{2e_{ii}E_i}{Z_2}. \quad (3)$$

2.2. Numerical Model - Calculation of the Temperature Distribution

Acoustic heating occurs when the sound field produced by the transducer is absorbed by the tissue. For an ultrasound traveling wave, the volumetric heat generation rate (Q_{ext} , W/m^3) is proportional to both the tissue's absorption and the intensity of the sound,

$$Q_{ext} = 2\alpha I, \quad (4)$$

where α is the acoustic absorption coefficient (Np/m), I is the radiated power density pattern (intensity) computed using equation (1). Throughout this paper, tissue absorption is assumed to equal tissue attenuation. In the proposed model, the temperature distribution is computed through a solution of the Pennes bio-heat equation [6],

$$\delta_t \rho c \frac{\partial T}{\partial t} = k \nabla^2 T - \rho_b w_b c_b (T_b - T) + Q_{meta} + Q_{ext}. \quad (5)$$

Here δ_t is a time-scaling coefficient = 1s, ρ is the tissue density (kg/m^3), c is the specific heat of tissue ($J/kg.K$). k is the tissue's thermal conductivity ($W/m.K$). On the right hand side of the equation, $\rho_b w_b c_b (T_b - T)$ is a source term accounting for blood perfusion. ρ_b is the density of blood. c_b is the specific heat of blood. w_b is the blood perfusion rate (1/s). T_b is the arterial blood temperature (assumed to equal $37^\circ C$). Q_{meta} (the heat source from metabolism (W/m^3)) is neglected since it is small. Table (I) shows the values for the thermal and acoustic parameters for the selected human tissues used in the simulations [7].

The COMSOL Multiphysics program (Royal Institute of Technology in Stockholm, Sweden) was used to compute the temperature spatial distribution at the nodes of a 2-D finite element mesh. Fig. 2 shows a schematic of the geometric mesh of the three different tissues (skin, tumor and breast) used in the computational model. The temperature distribution simulations were computed at three different frequencies of 0.75, 1.5 and 2.75 MHz and were allowed to run from 180 seconds up to 300 seconds (with a time step of 10 seconds). Boundary conditions were assumed to equal $37^\circ C$ at the edge of the problem space while those at the interface between the skin and the transducer were set to $10^\circ C$.

2.3. Analytical Model - Calculation of Temperature

The average energy dissipation, dE , in a cycle per unit length of a plane wave is expressed in the form [5],

$$dE = \text{Re} \left[\frac{pv^*}{2} \right] dx dy, \quad (6)$$

where p is the pressure, v^* is the complex conjugate of the velocity, and "Re" implies the real part of the expression. The average energy loss, E_{loss} , in a cycle per unit volume is,

$$E_{loss} = \alpha \text{Re}[pv'] \quad (7)$$

Then, the modified heat transfer equation is,

$$\rho c_p \frac{\partial T}{\partial t} = \nabla \cdot (k_h \nabla T) + q, \quad (8)$$

where ρ is the density of the material, c_p is the specific heat, T is the temperature, t is the time current, k_h is the heat conductivity, and q is the acoustic energy dissipation per volume in unit time, which is expressed as E_{loss} defined in (7). Since the temperature field is only considered in a short time, the heat conduction effect is small enough to be ignored. Thus, the temperature rise associated with the energy loss can be approximated as,

$$T = \frac{\alpha \text{Re}[pv']}{\rho C_p} t \quad (9)$$

The modified equation (8) has been solved to evaluate heating patterns in the tissues and tumor at various times during and after focused ultrasonic exposures. First, the intensity of the radiated power density of the ultrasonic wave is calculated by solving equation (1) using Matlab programming software. Second, the pressure p is computed by plugging I in the following equations:

$$I = \alpha \frac{p^2}{\rho c} \quad (10)$$

Thus,

$$p = \pm \sqrt{\frac{I \rho c}{\alpha}} \quad (11)$$

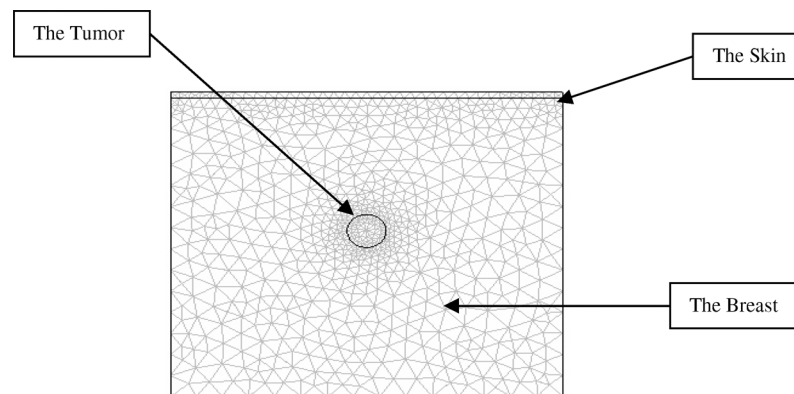


Fig. 2. Schematic diagram of the geometrical mesh used in the computations

TABLE I
Thermal and acoustic parameters for selected human tissues [7]

Tissue type	Thermal conductivity K=w/m/ °C	Density ρ (kg/m ³)	Phase velocity C (m/s)	Characteristic impedance Z=kg/m ² /s	Attenuation Coefficient (α) at 1MHz (dB/cm)	Specific heat (j/kg °C)
Tumor	0.5	1050	1540	1.63×10^6	0.7	3600
Skin	0.2	1200	1566	1.67×10^6	0.15	3600
Breast	0.5	1020	1510	1.38×10^6	0.22	3770
PZT	1.45	7500	4000	3.00×10^6	0.002	3400
Blood	0.6	1000	1500	1.50×10^6	0.2	4200

TABLE II
Numerical and analytical results at different frequencies and simulation times

Frequency MHz	Numerical Model			Analytical model		
	Skin	Breast	Tumor	Skin	Breast	Tumor
0.75 MHz	35.15 °C	39.15 °C	42.6 °C	8.66 °C	13.277 °C	28.93 °C
1.5 MHz	37.15 °C	41.15 °C	45.5 °C	37.417 °C	35.637 °C	47.77 °C
2.75 MHz	38.15 °C	47.15 °C	51.049 °C	58.77 °C	71.92 °C	83.5 °C

3. Results

3.1. Analytical Model

In the case of employing a therapeutic transducer at a frequency of 0.75 MHz as shown in Table 2, it is observed that the reasonable heat or temperature to destroy the cancerous cells is not enough. On the other hand, when employing the therapeutic transducer at a frequency of 1.5 MHz, Table 2, it is observed that the acceptable time range to destroy the cancerous cells without damage to the surrounding healthy tissues is in the range from 180 s up to 300 s. In addition, the temperature in the skin tissue increased, due to its small thickness as compared to the thickness of surrounding tissues. Thus, a bolus of degassed water of temperature (10°C) is placed on the skin as a cooling function to avoid burning of the skin. Moreover, when employing a therapeutic transducer at a frequency of 2.75 MHz, Table 2, the temperature in the regions of interest is shown to increase rapidly. Thus, increasing the frequency of simulation caused an increase in the absorption rate and the heat generation. The skin or even the breast tissue will be extremely over heated and this may cause tissue denaturing.

3.2. Numerical Model

The spatial temperature distribution in a multi-tissue arrangement is computed at three different frequencies and simulation times (Table 2). Fig. 3 shows a contour plot of the temperature distribution in the skin, breast and tumor tissues at 0.75 MHz at the end of 180 seconds. The maximum temperature (hot spot) occurred in the tumor and decreased when moving farther in other tissues. Increasing the time allowed for ultrasound therapy up to 300 s raised the temperature observed in the tumor and the surrounding tissues (Fig. 4). The temperature distribution, employing a therapeutic transducer at a higher frequency of 1.5 MHz, at the end of 180 seconds and 300 seconds ultrasound therapy is shown in Figs. 5 and 6. The highest temperature observed in the tumor was 45.5°C which is suitable for destroying cancerous cells without a noticeable damage to the surrounding tissues.

Simulation results using a transducer at a frequency of 2.75 MHz and at the end of 180 seconds and 300 seconds respectively is illustrated in Fig. 7 and Fig. 8. It is observed that the temperature predicted in the tumor is about 51.04 °C. The surrounding area near the tumor has been affected by higher temperatures compared to previous simulation results at lower frequencies. Increasing the time allowed for ultrasound raised the temperature of the tumor as well as the surrounding tissues. This rise in the temperature of the surrounding healthy tissue leads to their destruction, which is a drawback of the therapeutic process. In addition, the temperature distribution is observed to be more localized, thus indicating better transducer focusing capabilities at higher frequencies. Numerical computations and analytical calculations of temperatures in various tissues are summarized in Table II. A good agreement was only observed at a frequency of 1.5 MHz.

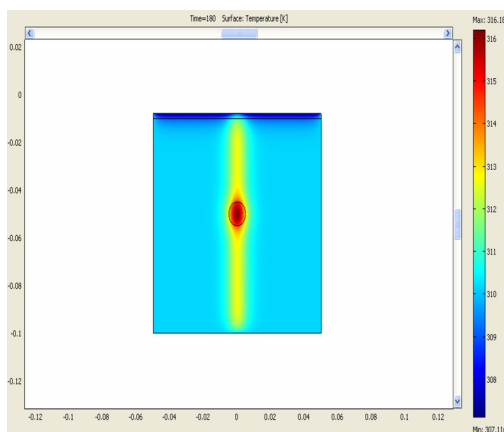


Fig. 3. Contour plot of the temperature fields in target areas at a frequency of 0.75 MHz and at a run time of 180s.

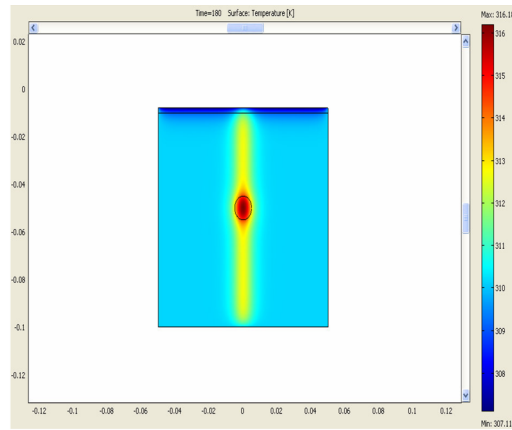


Fig. 4. Contour plot of the temperature fields in target areas at a frequency of 0.75 MHz and at a run time of 300s.

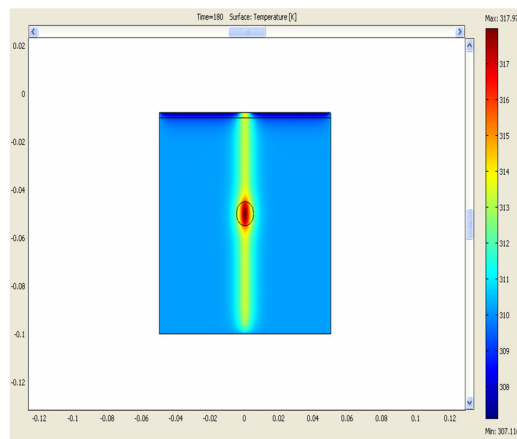


Fig. 5. Contour plot of the temperature fields in target areas at a frequency of 1.5 MHz and at a run time of 180s.

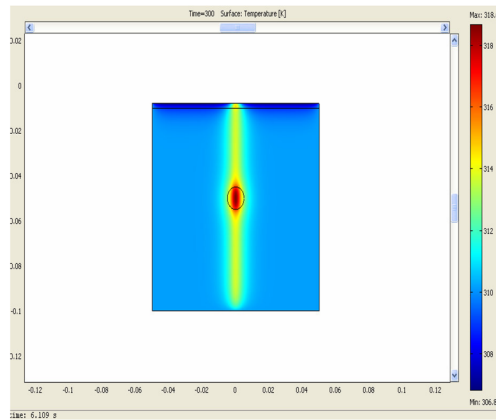


Fig. 6. Contour plot of the temperature fields in target areas at a frequency of 1.5 MHz and at a run time of 300s.

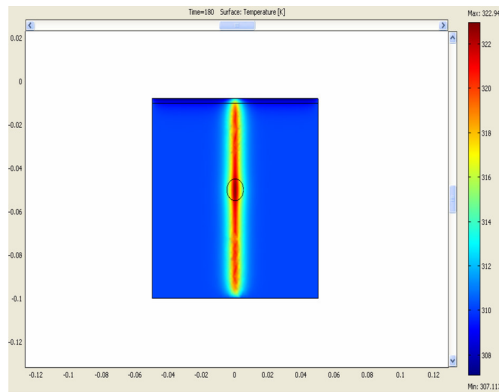


Fig. 7. Contour plot of the temperature fields in target areas at a frequency of 2.75 MHz and at a run time of 180s.

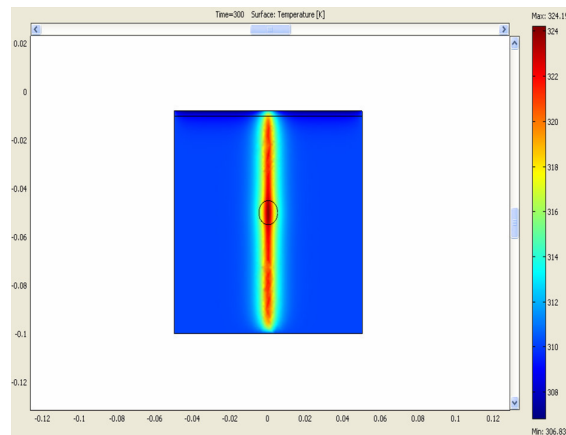


Fig. 8. Contour plot of the temperature fields in target areas at a frequency of 2.75 MHz and at a run time of 300s

4. Discussion

The purpose of this study was to numerically simulate the interaction of therapeutic ultrasound with a multi-tissue system at three different frequencies and stimulation times and to develop an analytical model to predict the sound field radiated by an ultrasonic transducer (a circular disk), calculate the temperature in different tissues. Numerical simulations are compared with analytical results.

An elevation in the temperature (hot spot) of the skin tissue was observed in all computations. Thus, a bolus of degassed water of temperature 10 °C is used as a cooling system in farther simulations. It acts as a heat sink, so as to avoid any pain or burning of the skin.

In order to calculate the temperature field in the multi-tissue system, the uniform pressure of ranges from 0.045 MPa to 0.0354 MPa is assumed to be applied on the surface of the breast tissue at the time from 180s to 300s, so the spatial temperature profiles are very similar for both solutions.

The numerical results show that employing a transducer at a frequency of 1.5 MHz is the most suitable for a successful ultrasound therapy. At this frequency, the highest temperature observed in the tumor was 45.5°C which is favorable for destroying cancerous cells without a noticeable damage to the surrounding tissues. On the other hand, analytical results show that the highest temperature predicted in the tumor was 47.77°C. The two solutions are considered in good agreement. The difference between the two solutions is minimized when a lower thermal conductivity value (e.g. k less than 0.5 W/m °C) for the tumor in the FEM computations is used. The discrepancy between the numerical and analytical results is more noticeable at the two other frequencies. This is caused by the fact that heat conduction is ignored in the analytical method. As the frequency of simulation increases, the ultrasound intensities increases and the specific absorption rate increases. Thus, the heat generation in tissues is increased, and the surrounding area near the tumor has been affected by higher temperatures, but the temperature distribution is more localized, as shown in Figs. 7 and 8.

5. Conclusions

The experimental study of the interaction of therapeutic ultrasound with biological tissues and the monitoring of the temperature distribution is a very expensive and difficult task. Thus, numerical modeling of ultrasound hyperthermia treatment at different simulation frequencies and therapy durations is a very important therapeutic demand. A model – based analysis of the interaction of ultrasound intensity with breast tissue including a tumor was carried out in an effort to predict the path of the sound waves and the temperature field in the regions of interest. Numerical and analytical calculations of temperature in various tissues were in good agreement at a certain frequency of 1.5 MHz. The computed results form a foundation for a better understanding of the interaction of ultrasound with biological tissues. More complex and extensive analytical methods including all aspects of heat conduction and wave attenuation should be considered in the future.

References

- [1] F.L. Lizzi and M. Ostromgilsky, “Analytical modeling of ultrasonically induced tissue heating,” *Ultrasound Med Biol.*, vol. 13, no. 10, pp. 607-18, 1987.
- [2] H.H. Pennes, “Analysis of tissues and arterial blood temperatures in the resting human forearm,” *J. Appl. Physiology*, vol. 85, no. 1, pp. 5-34, 1998.
- [3] F. Feng, A. Mal, M. Kabo, J.C.Wang, “The mechanical and thermal effects of focused ultrasound in a model biological material”, *J Acoust Soc Am.*, vol. 117, pp. 2347-55, 2005.
- [4] B.-Y. lu, R.-S. Yang, W.-L. Lin, K.-S. Cheng, T.-S. Kuo, “Theoretical study of convergent ultrasound hyperthermia for treating bone tumor,” *Med Eng Phys.*, vol. 22, no. 4, pp. 253-63, 2000.
- [5] Y. Kagawa, K. Takeuchi, T. Yamabuchi, “A simulation of ultrasonic hyperthermia using a finite element model,” *IEEE Trans Ultrason Ferroelectr Freq Control*, vol. 33, no. 6, pp. 765-77, 1986.
- [6] P.M. Meany, R.L. Clarke, G.R. Ter Haar, I.H. Rivens, “A 3-D finite-element model for computation of temperature profile and regions of thermal damage during focused ultrasound surgery exposures,” *Ultrasound in Medicine and Biology*, vol. 24, no 9, pp. 1489-1499, 1998.
- [7] K.L. Gentry, M.L. Palmeri, and N. Sachedina, S.W. Smith, “Finite-element analysis of temperature rise and lesion formation from catheter ultrasound ablation transducers,” *IEEE Trans Ultrason Ferroelectr Freq Control*, vol. 52, no. 10, pp. 1713-21, 2005.
- [8] D. A. Christensen, *Ultrasonic Bioinstrumentation*, New York: Wiley, 1988.